Int J Thermophys (2008) 29:1555–1566
DOI 10.1007/s10765-007-0350-4

Uncertainty Analysis of Evaporation Rate in Magnetic Suspension Balance/Diffusion-Tube Humidity Generator

H. Abe · H. Tanaka · H. Kitano

Published online: 16 January 2008

Abstract An analysis method for the uncertainty of a small evaporation rate in a magnetic suspension balance/diffusion-tube humidity generator has been developed. Using experimentally obtained data, the uncertainty is evaluated as a function of measurement time. It is found that the observed standard deviation of the evaporation rate in a region of short measurement time (short term) is inversely proportional to the measurement time, and that in a region of long measurement time (long term) the standard deviation does not vary markedly with increasing measurement time. The behavior of the observed standard deviation in the short term is attributable mainly to the uncertainty of the balance reading, and that in the long term to the variability of room temperature. The results of the investigation show that the use of only least-squares analysis leads to underestimation of the uncertainty.

Keywords Calibration gas · Cavity ring-down spectroscopy · Gas standard · Humidity standard · Trace moisture

1 Introduction

The measurement of trace moisture in process gases has become increasingly important in the semiconductor industry because it has been recognized that even trace amounts of water vapor can adversely affect the yield and product quality of semiconductor devices [1]. Various measuring instruments to detect trace moisture in gases have been developed [2]. The choice of the instrument may depend on factors such as humidity range, response time, size, and cost. Regardless of the type of instrument chosen, periodic calibrations are always needed to achieve reliable measurements.

H. Abe (✉) · H. Tanaka · H. Kitano
National Metrology Institute of Japan (NMIJ), AIST, Tsukuba Central 3, Tsukuba 305-8563, Japan
e-mail: abe.h@aist.go.jp

Diffusion-tube and permeation-tube [3] humidity generators (DTGs and PTGs) are commonly used for such a purpose because these generators can relatively easily realize humidity standards in the trace moisture region. In a DTG or a PTG, a diffusion cell (consisting of a small water vessel having a diffusion tube) or a permeation tube is placed in a chamber to be used as the source of water vapor. The water vapor from the source is mixed with a dry gas in the chamber, and a humid gas is generated. The amount-of-substance fraction of water in the gas, x_{w}, produced in this manner is given by

$$x_{\mathrm{w}} = \frac{N + N_{\mathrm{b}} + F x_{\mathrm{b}}}{N + N_{\mathrm{b}} + F} \approx \frac{N}{F} + \frac{N_{\mathrm{b}}}{F} + x_{\mathrm{b}}, \tag{1}$$

where N is the amount-of-substance of water vapor evaporated per unit time from the diffusion cell (molar evaporation rate) or permeation tube (molar permeation rate), N_{b} is the amount-of-substance of water vapor adsorbed/desorbed per unit time from the inside surfaces of the chamber and pipes, F is the molar flow rate of the dry gas, and x_{b} is the amount-of-substance fraction of residual moisture in the dry gas. Equation 1 shows that the uncertainty analysis of N is an essential issue for realizing primary standards with DTGs or PTGs. In this article, we focus only on the uncertainty of N; we are not concerned here with the uncertainties of N_{b}, F, and x_{b}.

N is related to the evaporation rate q_{e} of water vapor from the diffusion tube or permeation tube by

$$q_{\mathrm{e}} = N M_{\mathrm{w}}, \tag{2}$$

where M_{w} is the molar mass of water, and its value is known with much smaller relative uncertainty than that of N dealt with in this article. Therefore, the uncertainty of q_{e} is given by

$$u^2(q_{\mathrm{e}}) = u^2(N) M_{\mathrm{w}}^2 + u^2(M_{\mathrm{w}}) N^2 \approx u^2(N) M_{\mathrm{w}}^2, \tag{3}$$

where $u(X)$ is the standard uncertainty of the quantity X. Equation 3 shows that the analysis of $u(N)$ is essentially the same as that of $u(q_{\mathrm{e}})$. The quantity q_{e} can be measured by weighing the diffusion cell or permeation tube either periodically or continuously using an analytical balance. Details of the methods of measuring q_{e} and its uncertainty analysis are found in the literature [4–6], which gives us helpful examples to realize humidity standards using DTGs and PTGs. However, it seems that further studies are still necessary to measure q_{e} more accurately and precisely, and to evaluate $u(q_{\mathrm{e}})$ more accurately if the value of q_{e} is very small, for instance, $q_{\mathrm{e}} \sim 10\,\mu\mathrm{g}\cdot\mathrm{h}^{-1}$ to attain $x_{\mathrm{w}} \sim 10\,\mathrm{nmol}\cdot\mathrm{mol}^{-1}$. In such a case, even a small drift in the balance reading caused by various environmental effects can be a major component of the uncertainty. Furthermore, it normally takes a long time to determine such a small q_{e} by mass measurement, and it is difficult to maintain the same experimental conditions during the experiment. Therefore, the environmental effects on the balance and moisture generation should be quantitatively evaluated in more detail.

In this study, we performed consecutive measurements of a mass-change rate ($\approx$11 $\mu g \cdot h^{-1}$) for 14–31 days using a magnetic suspension balance/diffusion-tube humidity generator (MSB/DTG) to examine the environmental effects on the balance reading and trace-moisture generation. The effect of the variability of room temperature on q_e was quantitatively evaluated using the MSB and a moisture analyzer (MA) based on cavity ring-down spectroscopy [7–9]. The relationship between $u(q_e)$ and measurement time was studied. An analysis method of $u(q_e)$ for small q_e in the MSB/DTG was developed.

2 Experimental

The experimental apparatus used in this work was essentially the same as that described in our previous article [10]. Dry nitrogen (N_2) gas was prepared using a purifier (Saes Getters, Monotorr PS4-MT3-N-1). The amount-of-substance fraction of water vapor in the gas was estimated to be below 1 $nmol \cdot mol^{-1}$. This dry gas was introduced into the inlet of a generation chamber and a bypass line using two thermal mass flow controllers (Stec, SEC-F440M). The total flow rate was maintained at 2.5 $L \cdot min^{-1}$ or 20 $L \cdot min^{-1}$, and the flow rate to the chamber was 0.1 $L \cdot min^{-1}$; the flow rates in $L \cdot min^{-1}$ used in this paper correspond to those measured under the standard conditions of 101.325 kPa and 0°C. Inside the chamber, a diffusion cell [11] was suspended from the measuring load of an MSB (Rubotherm). Water was stored in the diffusion cell, and water vapor that evaporated through the diffusion tube was diluted with dry N_2 gas coming from the inlet. Humid gas generated in this manner was taken from the outlet of the chamber. The line from the outlet was connected to the bypass line, and the humid gas was mixed and diluted with the dry N_2 gas. This mixed flow was divided into two streams. One was introduced into a pressure regulator (PR) to control the pressure inside the chamber, which was maintained at 150 kPa. The other was led to an MA (Tiger Optics, MTO-1000-H_2O) based on cavity ring-down spectroscopy to monitor the amount-of-substance fraction of water in the humid gas generated.

The mass-change rate of the diffusion cell was measured with the MSB. Mass data were collected every 2 or 3 min. The zero-point correction and calibration of the MSB were performed every 10 or 12 min and every 30 or 40 min, respectively. The temperature of the chamber was maintained at 25°C by monitoring the temperature with a platinum resistance thermometer (PRT). Atmospheric pressure was measured with a digital manometer (Yokogawa, MT210). The temperature and relative humidity near the MSB were measured with a PRT and a humidity sensor (Sato Keiryoki, SK-L200TH), respectively. The data of pressure, temperature, humidity, and flow rate were collected every 1 min using a personal computer.

3 Uncertainty Analysis

We consider the standard uncertainty of the evaporation rate $u(q_e)$ as a function of the measurement time Δt_m in line with [12]. The uncertainty due to the calibrations of instruments is negligible, and is not further considered in this article.

3.1 Formulation of Uncertainty

q_e is measured as the mass-change rate of the diffusion cell q_m (≤ 0) using the relation,

$$q_e = -q_m. \tag{4}$$

The change in mass of the diffusion cell is given by $-q_m t$ where t is the time. Hence, q_m is given by

$$q_m = -\frac{m_0 - R}{t} = -\frac{1}{t}\left(m_0 - r\frac{1-\rho_a/\rho_0}{1-\rho_g/\rho}\right), \tag{5}$$

where m_0 is the initial mass of the diffusion cell, R is the buoyancy-corrected reading [13], r is the MSB reading, ρ_a is the air density, ρ_0 is the density of the reference mass for balance calibration, ρ_g is the gas density inside the chamber, and ρ is the density of the diffusion cell. In this study, q_m is estimated using a least-squares fit with a linear function. The output estimate of mass-change rate and its uncertainty obtained using the fit are denoted as q_f and $u(q_f)$, respectively. $u(q_f)$ is not necessarily the same as $u(q_e)$ because, in the least-squares analysis, $u(q_f)$ is calculated from the residuals with respect to the fitted line on the assumption that the residuals are randomly scattered about the true line. However, when the Δt_m used for the fit is small, the residuals may not accumulate sufficient information on the true value, as schematically illustrated in Fit 1 ($\Delta t_m = \Delta t_1$) in Fig. 1. In this case, q_f deviates from the true value q_m, and $u(q_f)$ represents only the uncertainty of the fit with regard to the inaccurately determined q_f. In order to consider this effect quantitatively, we rewrite q_m in the form,

$$q_m = q_f + \Delta q_f, \tag{6}$$

where $\Delta q_f = q_m - q_f$. The expectation of the additive correction Δq_f is zero. Using Eqs. 4 and 6, $u(q_e)$ is given by

$$u^2(q_e) = u^2(q_f) + u^2(\Delta q_f). \tag{7}$$

According to the discussion in Annex E in [12], $u(\Delta q_f)$ is expressed by

$$u(\Delta q_f) \equiv s(\Delta q_f) = s(q_f) = \sqrt{\frac{1}{n-1}\sum_{i=1}^{n}(q_{fi} - \bar{q}_f)^2}, \tag{8}$$

where q_{fi} represents q_f obtained from the ith measurement, $\bar{q}_f$ is the average of the n measurements, and $s(X)$ is the experimental standard deviation of X. Therefore, we can determine $s(q_f)$ using Eq. 8 and experimentally obtained q_{fi}. Using Eqs. 7 and 8, we obtain

$$u^2(q_e) = u^2(q_f) + s^2(q_f). \tag{9}$$

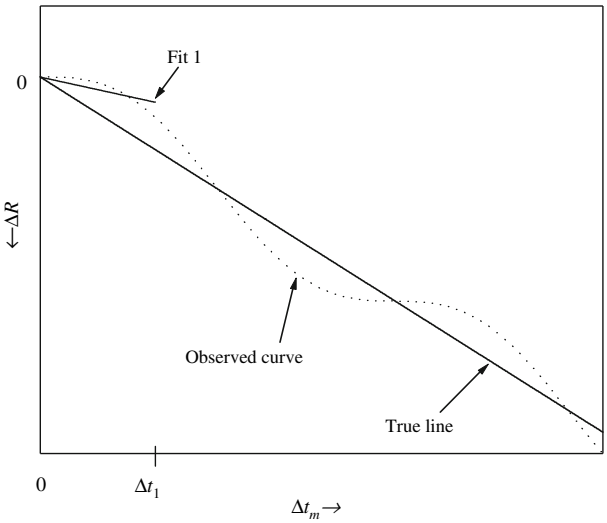

Fig. 1 Schematic of the true line and fitting line is shown. Fit 1 is obtained by least-squares analysis with the measurement time $\Delta t_{\mathrm{m}} = \Delta t_1$. Fit 1 may deviate greatly from the true line when Δt_1 is small

3.2 Analysis of Experimental Data

$s(q_{\mathrm{f}})$ depends on the measurement time Δt_{m}, and a similar technique to that employed in Knopf's paper [14] was used to calculate $s(q_{\mathrm{f}})$ at Δt_{m}, as described below. The mass measurement of the diffusion cell was performed consecutively for 18 days starting in September 2005 (Experiment I). Only a portion of the data of the first 80 h is shown in Fig. 2. Values in the figure are differences from the initial mass. The data were divided using a time window of 24 h ($\Delta t_{\mathrm{w}} = 24\,\mathrm{h}$) as illustrated in the figure, and 18 sets of data were generated. Each set of data was used to determine $q_{\mathrm{f}i}$ using a least-squares fit with a linear function. As a result, 18 mass-change rates were obtained. Using these data, we obtained $\bar{q}_{\mathrm{f}} = 11.64\,\mu\mathrm{g}\cdot\mathrm{h}^{-1}$ and $s(q_{\mathrm{f}}) = 0.07\,\mu\mathrm{g}\cdot\mathrm{h}^{-1}$ for $\Delta t_{\mathrm{w}} = 24\,\mathrm{h}$. Time windows other than 24 h in the range of 3–100 h were also examined using the same data. The results are shown in Fig. 3a. A similar experiment was performed for 31 days in April 2006 (Experiment II), as shown in Fig. 3b. In both experiments, $s(q_{\mathrm{f}})$ decreases with increasing Δt_{w} in the short-term region of Δt_{w}. Over the longer term, the $s(q_{\mathrm{f}})$ values appear to converge at approximately $0.03\,\mu\mathrm{g}\cdot\mathrm{h}^{-1}$ in Experiment I, and at $0.15\,\mu\mathrm{g}\cdot\mathrm{h}^{-1}$ in Experiment II.

The behavior in the long-term region is attributable to an environmental effect on trace-moisture generation. It was found that the variability of room temperature affects the evaporation rate even though the temperature of the chamber is maintained constant. When the room temperature varied by ΔT_{r}, the change in the evaporation rate was observed to be $C\,\Delta T_{\mathrm{r}}$, where C is the sensitivity coefficient. We determined C using evaporation rates measured at various room temperatures. This experiment was performed consecutively for 14 days. Room temperature was variously maintained near 25, 31, 23, and 25°C with the use of an air conditioner. The evaporation rates were determined using a time window of 10 h. The mass data recorded during the transitions

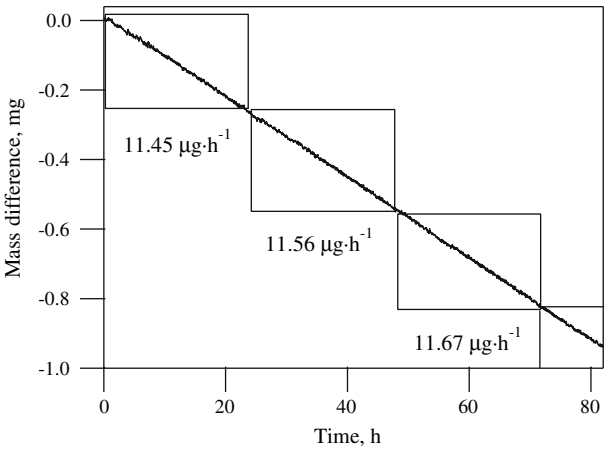

Fig. 2 A portion of the data of the first 80 h in Experiment I is shown. The data are divided using a time window of 24 h. Each set of the data is used to determine an evaporation rate using a least-squares fit with a linear function

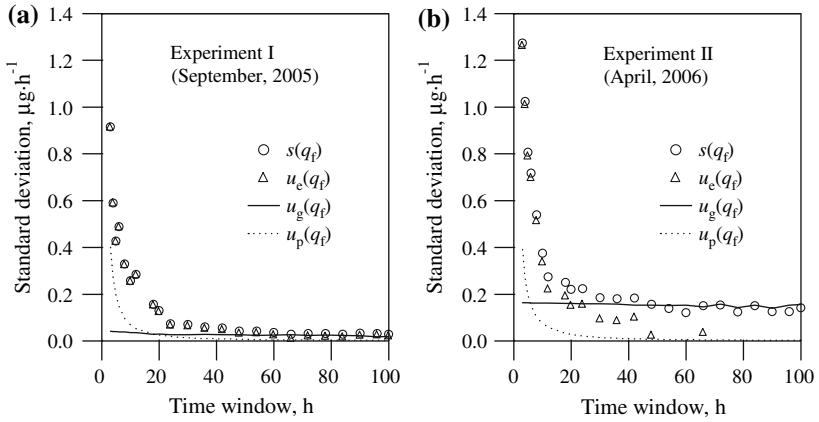

Fig. 3 Standard deviation as a function of the time window is shown. $s(q_f)$ is the observed standard deviation of evaporation rates, $u_e(q_f)$ is the standard uncertainty due to balance reading, $u_g(q_f)$ is the standard uncertainty due to variability of room temperature, and $u_p(q_f)$ is the pooled standard uncertainty calculated using results of least-squares analysis

of room temperature were not used for the analysis because they did not give constant mass-change rates. Figure 4a shows the result of the experiment. Using a least-squares fit with a linear function, we obtain $C = 0.142\,\mu g \cdot h^{-1} \cdot K^{-1}$. The amount-of-substance fraction of water in the gas, x_w, was also monitored using the MA at the same time, as shown in Fig. 4b. During the experiment, the total flow rate of the dry gas F was maintained constant. Therefore, we could also calculate the sensitivity coefficient using x_w, F, and room temperature T_r. The result was $C = 0.132\,\mu g \cdot h^{-1} \cdot K^{-1}$. These two values obtained experimentally separately are in agreement. Using the average of the two values, we finally obtain $C = 0.14\,\mu g \cdot h^{-1} \cdot K^{-1}$. The standard

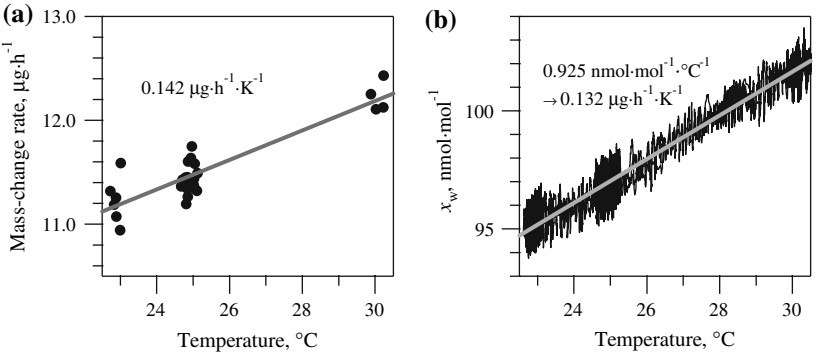

Fig. 4 Effect of room temperature on the evaporation rate and the generated trace moisture is shown. Value of the sensitivity coefficient C obtained using data measured with the MSB was 0.142 $\mu g \cdot h^{-1} \cdot K^{-1}$ and that with the MA was 0.132 $\mu g \cdot h^{-1} \cdot K^{-1}$, shown in Fig. 4a and b, respectively

deviation of room temperature $s(T_r)$ was approximately 0.2 K in Experiment I, and $Cs(T_r) = 0.03\,\mu g \cdot h^{-1}$ is probably responsible for $s(q_f)$ in the long-term region. This interpretation is consistent with the results of Experiment II; the standard deviation of room temperature was approximately 1.1 K, giving $Cs(T_r) = 0.15\,\mu g \cdot h^{-1}$.

Thus, $s(q_f)$ is further divided as

$$s^2(q_f) = u_g^2(q_f) + u_e^2(q_f), \tag{10}$$

where $u_g(q_f)$ expresses the standard uncertainty due to the variability of trace-moisture generation caused by the variability of room temperature described above, $u_e(q_f)$ is the standard uncertainty due to the other environmental effects, and the correlation between these two terms is assumed to be negligible. $u_g(q_f)$ is given by $Cs(T_r)$. Therefore, $u_e(q_f)$ is expressed by

$$u_e(q_f) = \sqrt{s^2(q_f) - C^2 s^2(T_r)}. \tag{11}$$

$u_g(q_f)$ given by $Cs(\bar{T}_r)$ and $u_e(q_f)$ calculated using Eq. 11 are shown in Fig. 3a and b, where the average temperature of each measurement, $\bar{T}_r$, was used to calculate $s(T_r)$. The figures show that the behavior of $s(q_f)$ in the short-term Δt_w region is attributable to $u_e(q_f)$. The pooled uncertainty of the fitting of $u_p(q_f)$ calculated using

$$u_p^2(q_f) = \frac{\sum_{i=1}^{n} \nu_i u^2(q_{fi})}{\sum_{i=1}^{n} \nu_i}, \tag{12}$$

is shown in Fig. 3a and b for comparison, where $u(q_{fi})$ represents the standard uncertainty of q_{fi} obtained from the least-squares analysis and ν_i is the degrees of freedom. Ideally, $u_p(q_f)$ represents the uncertainty of the evaporation rate, and should become comparable to $u_e(q_f)$ when $u_g(q_f)$ is negligible. However, in Experiment I in which $u_g(q_f)$ is much smaller than $u_p(q_f)$ and $u_e(q_f)$ in the short-term Δt_w region, $u_p(q_f)$

was smaller than $u_e(q_f)$, indicating that $u_p(q_f)$ inadequately expresses the uncertainty, because of the reliance on residuals that do not incorporate sufficient information for reliable fitting. Furthermore, in the long-term Δt_w region, $u_p(q_f)$ could not be used to explain the observed variability of the evaporation rate stemming from the variability of room temperature. The results of the analysis show that information on $u_g(q_f)$ and $u_e(q_f)$ are necessary to accurately evaluate the uncertainty of the evaporation rate.

3.3 Uncertainty of Evaporation Rate

In this section, we consider two cases in which a measuring instrument is calibrated against q_f. The uncertainty is evaluated using the experimental data as a function of the measurement time Δt_m. The procedure for determining the standard uncertainty of the evaporation rate, $u(q_e)$, depends on the ratio of the period of time used to calibrate the instrument Δt_c, namely, the ratio of Δt_c to Δt_m. In the calibration, the average of the indication of the instrument $\bar{I}$ measured during Δt_c is compared with x_w determined using q_f. If multiple calibrations are performed during Δt_m or only a small part of Δt_m is used as Δt_c for the calibration, referred to as case (i), it is considered that the calibration is performed against q_f with an uncertainty of $\sqrt{u_p^2(q_f) + u_g^2(q_f) + u_e^2(q_f)}$. Thus, using Eqs. 9–11, the uncertainty is given by

$$u(q_e) = \sqrt{u_p^2(q_f) + C^2 s_p^2(T_r) + s^2(q_f) - C^2 s^2(\bar{T}_r)}, \tag{13}$$

where $s_p(T_r)$ is the pooled standard deviation of the room temperature calculated in a similar manner to that described in Eq. 12. If $\Delta t_c = \Delta t_m$, referred to as case (ii), it is considered that the calibration is performed against q_f with an uncertainty of $\sqrt{u_p^2(q_f) + u_e^2(q_f)}$ at the average room temperature during the calibration. Therefore, the uncertainty is expressed by

$$u(q_e) = \sqrt{u_p^2(q_f) + s^2(q_f) - C^2 s^2(\bar{T}_r)}. \tag{14}$$

The $u(q_e)$ values for cases (i) and (ii) calculated using the time windows are shown in Fig. 5a and b, respectively. $u_p(q_f)$ is also shown in Fig. 5a and b for comparison. The $u(q_e)$ values were determined using statistical information, namely, $s(q_f)$ and $s(\bar{T}_r)$, obtained from multiple divided data recorded for 18 days or 31 days. Thus, the values are not exactly the same as $u(q_e)$ for a single measurement with a measurement time of Δt_m. However, we can examine the statistical behavior of $u(q_e)$ with a measurement time of Δt_m by considering $u(q_e)$ at a time window of Δt_w in Fig. 5a and b as the estimate for a single measurement with a measurement time of $\Delta t_m = \Delta t_w$. Figure 5a and b shows that the use of only least-squares analysis leads to an underestimation of uncertainty. As stated above, information on $u_g(q_f)$ and $u_e(q_f)$ is necessary to evaluate $u(q_e)$ accurately. In particular, $u_e(q_f)$ cannot be assessed from a single experimental data set. Therefore, $u_e(q_f)$ should be experimentally evaluated before or after the calibration, or a pooled value, which is reasonable and acceptable, should be used. When

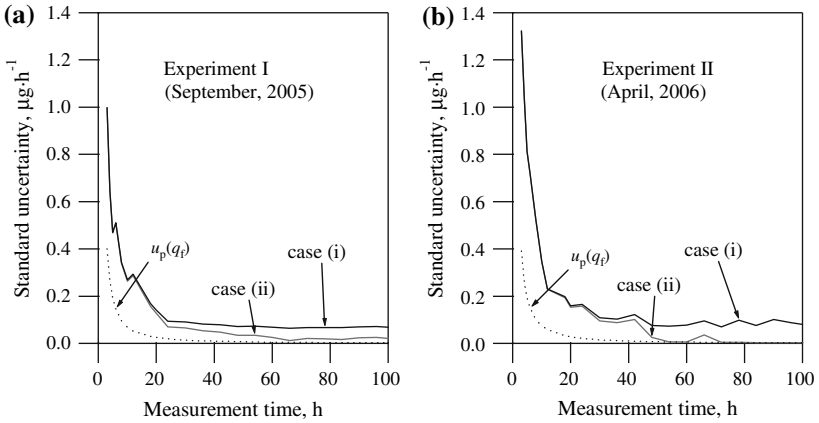

Fig. 5 Standard uncertainties as a function of the measurement time for (**a**) Experiment I and (**b**) Experiment II are shown. Two procedures were considered for determining the standard uncertainty of the evaporation rate, which are labelled as cases (i) and (ii) in the figure (see text). $u_p(q_f)$ is the pooled standard uncertainty obtained from least-squares analysis

the pooled value $u_{ep}(q_f)$ is available, the following equations should be used:

$$u(q_e) = \sqrt{u^2(q_f) + C^2 s^2(T_r) + u_{ep}^2(q_f)} \tag{15}$$

and

$$u(q_e) = \sqrt{u^2(q_f) + u_{ep}^2(q_f)}, \tag{16}$$

where Eq. 15 is for case (i) and Eq. 16 is for case (ii); $s(T_r)$ is the standard deviation of room temperature during the measurement.

4 Discussion

Figure 3a and b shows that $u_e(q_f)$ decreases with increasing $\Delta t_w (= \Delta t_m)$. A least-squares analysis of $u_e(q_f)$ using a function $B\Delta t_m^{\alpha}$ gives $\alpha = -1.05$ ($B = 2.76\,\mu g$) for Experiment I and $\alpha = -1.06$ ($B = 4.22\,\mu g$) for Experiment II, where B and α are a constant factor and an exponent, respectively, indicating that $u_e(q_f)$ is likely to be inversely proportional to Δt_m. If we assume that the uncertainty in the measurement of time is negligible, there are two uncertainty components responsible for this Δt_m^{-1} behavior of $u_e(q_f)$: the uncertainty due to the variability of trace-moisture generation expressed other than by $Cs(T_r)$, and the uncertainty of the balance reading. It was found that the former could not explain the behavior. The variability of trace-moisture generation was evaluated using x_w measured with the MA. The value of x_w was converted to an evaporation rate at each measurement point using Eqs. 1 and 2 using the mean value of F, $N_b = 0$, and $x_b = 0$. Evaporation rates obtained in this manner were divided using the time windows, and the standard deviations of the mean evaporation rates were calculated as a function of Δt_m. These data were analyzed

similarly to that employed for $u_e(q_f)$, giving $B = 0.30\,\mu g$ and $\alpha = -0.46$ for Experiment I, and $B = 0.32\,\mu g$ and $\alpha = -0.10$ for Experiment II. The B values are approximately ten times smaller than those of $u_e(q_f)$ in Fig. 3a and b. Furthermore, a fraction of each value must originate from the variability of room temperature; the analysis of $Cs(T_r)$ produced $B = 0.05\,\mu g$ and $\alpha = -0.19$ for Experiment I, and $B = 0.17\,\mu g$ and $\alpha = -0.03$ for Experiment II. These results indicate that the Δt_m^{-1} behavior of $u_e(q_f)$ is attributable mainly to the latter, namely, the uncertainty of the balance reading.

We performed a simulation considering randomly distributed errors over constant mass-loss data. The observed Δt_m^{-1} behavior of $u_e(q_f)$ can be reproduced well using the model. If this model is correct, Eqs. 13 and 15 can be expressed using the constant factor A in the form,

$$u(q_e) = \sqrt{A^2 + B^2/\Delta t_m^2}, \tag{17}$$

where A (>0) is attributable to the uncertainty due to the variability of trace-moisture generation, and $B(>0)$ can be approximated by the same B as that used in the least-squares analysis, and attributable to the uncertainty of the balance reading. Equation 17 indicates that the choice of an adequately long Δt_m reduces the uncertainty. Equation 17 also implies that it is unnecessary to adopt Δt_m much greater than B/A. $u(q_e)$ does not greatly improve with increasing Δt_m in the region of long-term Δt_m, resulting from the nature of the function on the right-hand side of Eq. 17. For instance, the $u(q_e)$ values are $0.108\,\mu g \cdot h^{-1}$ at $\Delta t_m = 30\,h$, and $0.081\,\mu g \cdot h^{-1}$ at $\Delta t_m = 100\,h$ in case (i) in Fig. 5b; even though Δt_m in the latter is three times greater than that in the former, the improvement is only 0.27% at $q_e = 10\,\mu g \cdot h^{-1}$. B represents the magnitude of the environmental effects on the balance reading. As has already been reported, the B values are $2.76\,\mu g$ in Experiment I and $4.22\,\mu g$ in Experiment II. We calculated the B value using the data from the first 18 of the 31 days in Experiment II, and found it to be $4.53\,\mu g$. This indicates that the difference in B between Experiments I and II is not attributable to total measurement time. Typical environmental effects on balance reading are attributable to zero-point drift, change in scale interval, and change in buoyancy. In this study, these effects were compensated in both Experiments I and II using zero-point correction and calibration. However, B differed between the two experiments, indicating that there might be a residual uncertainty due to these effects and/or there might be uncertainty components of the balance reading other than those effects to be considered.

The least-squares analysis used to determine the value of the temperature sensitivity coefficient C showed very small fitting uncertainty (the relative standard uncertainty was $<0.8\%$). On the analogy of the uncertainty analysis of the evaporation rate in this article, this value is likely to insufficiently express the uncertainty of C. The fluctuation of the evaporation rate due to the variability of room temperature is probably attributable to heat transfer, which affects the evaporation rate. This means that C depends on various experimental conditions that relate to the heat transfer and affect the evaporation rate, such as the temperature of the chamber, the flow rate of dry gas to the chamber, the pressure inside the chamber, and air flows around the outside

of the chamber. Therefore, we need to examine the statistical behavior of C under various conditions to accurately evaluate the uncertainty of C; this research has not yet been performed. However, the temperature of the chamber, the flow rate of dry gas to the chamber, and the pressure inside the chamber, which probably predominantly determine the magnitude of C, were controlled in this study, which means that the uncertainty of C due to the changes in these conditions is expected to be small. Furthermore, the value of $s(q_f)$ observed in the long-term Δt_w region in Experiments I and II was reproduced well using the value of C determined independently of the two experiments. These facts suggest that an appropriate value of C was used to interpret the data in this study, although it was difficult to evaluate its uncertainty.

5 Conclusions

We studied the statistical behavior of the evaporation rate in the DTG measured using the MSB. It was found that the observed standard deviation of the evaporation rate in the short-term Δt_m region was inversely proportional to Δt_m. In contrast, in the long-term Δt_m region, the standard deviation did not vary markedly. Therefore, a suitable value of Δt_m should be chosen to reduce the uncertainty and to perform the experiment efficiently.

The variability of the room temperature might affect the temperature of the diffusion cell. This was probably because it was difficult to fully thermally insulate the inside of the chamber from the outside, although the temperature inside the chamber was controlled. Heat transfer from the outside can disturb water evaporation, and is a component of uncertainty of the evaporation rate. Hence, it is important to determine the value of C and to record the room temperature in the experiment; the uncertainty due to this effect should be quantitatively evaluated.

It is difficult to accurately assess the uncertainty of the evaporation rate by least-squares analysis using a single experimental data set. Furthermore, it was found that the use of only least-squares analysis leads to an underestimation of the uncertainty. Therefore, multiple data sets should be used to avoid these problems, and the statistical behavior of the evaporation rate should be analyzed to evaluate the uncertainty.

The value of $u_e(q_f)$ in the short-term Δt_m region was mainly attributable to the environmental effect on the balance reading, and in the long-term Δt_m region to the variability of room temperature. However, we have not yet found the exact causes of the uncertainty. Further study is needed to identify the causes and to develop a method of reducing $u_e(q_f)$.

The value of $s(q_f)$ at $\Delta t_m = 3\,\mathrm{h}$ observed in this work was $\approx 1\,\mu\mathrm{g}\cdot\mathrm{h}^{-1}$. This may be a negligible uncertainty component when $q_f \gg s(q_f)$, for instance, $q_f > 1{,}000\,\mu\mathrm{g}\cdot\mathrm{h}^{-1}$, and it may be unnecessary to consider $s(q_f)$ in detail in the uncertainty analysis. However, when $q_f \approx 10\,\mu\mathrm{g}\cdot\mathrm{h}^{-1}$, the analysis must be performed more carefully because even a small error in the analysis may significantly affect the interpretation of results obtained using an MSB/DTG.

Acknowledgments The authors wish to thank Dr. Chiharu Takahashi and Dr. Nobuaki Ochi for critically reading the article.

References

1. *International Technology Roadmap for Semiconductors* (2006) http://www.itrs.net/reports.html
2. H.H. Funke, B.L. Grissom, C.E. McGrew, M.W. Raynor, Rev. Sci. Instrum. **74**, 3909 (2003)
3. See, for example, A.-N. Nowak, P. Konieczka, A. Przyjazny, J. Namieśnik, Crit. Rev. Anal. Chem. **35**, 31 (2005); S. Tumbiolo, L. Vincent, J.-F. Gal, P.-C. Maria, Analyst **130**, 1369 (2005)
4. ASTM D 4298-95, *Standard Guide for Intercomparing Permeation Tubes to Establish Traceability* (ASTM International, United States, 1999)
5. ISO 6145-10, *Gas analysis-Preparation of calibration gas mixtures using dynamic volumetric methods-Part10: Permeation method* (International Organization for Standardization, Geneva, 2002)
6. ISO 6145-8, *Gas analysis-Preparation of calibration gas mixtures using dynamic volumetric methods-Part8: Diffusion method* (International Organization for Standardization, Geneva, 2005)
7. A. O'Keefe, D.A.G. Deacon, Rev. Sci. Instrum. **59**, 2544 (1988)
8. D. Romanini, K.K. Lehmann, J. Chem. Phys. **99**, 6287 (1993)
9. G. Berden, R. Peeters, G. Meijer, Int. Rev. Phys. Chem. **19**, 565 (2000)
10. H. Abe, H. Kitano, Sens. Actuators A: Phys. **136**, 723 (2007)
11. H. Abe, H. Kitano, Sens. Actuators A: Phys. **128**, 202 (2006)
12. ISO, *Guide to the Expression of Uncertainty in Measurement* (International Organization for Standardization, Geneva, 1995)
13. R. Schwartz, in *Comprehensive Mass Metrology*, ed. by M. Kochsiek, M. Gläser (Wiley-VCH, Berlin, 2000), p. 248
14. D. Knopf, Accred. Qual. Assur. **6**, 113 (2001)